Study of Coherent Properties of an Exciton in Semiconductor Quantum Dots

R.S. Kolodka*, I.P. Pundyk, I. Dmitruk

Physics Department, Taras Shevchenko National University of Kyiv, 2/1, Akademik Glushkov Prosp., 03127 Kyiv, Ukraine

In this paper, we make a review of experimental techniques used in the study of semiconductor quantum dots and focus on the basic principles of optical coherent control of the exciton. We discuss both optical methods of investigation (time-resolved pump-probe, control of *p*-shell by measuring the photoluminescence from *s*-level, resonant fluorescence) and a photocurrent technique. Although the last one reduces the coherence of the system, but gives a quantitative measure of it. Special attention is applied to physical properties of self-assembled quantum dots as the methods of production which allow obtaining high-quality nanoparticles in macroscopic quantities. We also discuss our results obtained from colloidal CdSe quantum dots photoluminescence and transmission measurements, and Raman scattering spectra. We witness Stokes shift for an ensemble of nanoparticles that have a fairly broad size distribution. The analysis of the secondary radiation of the CdSe nanoparticles was done to study both processes leading to this energy shift and the loss of exciton polarization.

Keywords: Quantum dots, Exciton, Nanoparticles, Coherent control, Relaxation.

DOI: 10.21272/jnep.12(3).03022

PACS numbers: 61.46.Df, 73.22.– f, 78.67.Hc

1. INTRODUCTION

Development of research methods in physics of semiconductors and semiconductor devices came along with a gradual decrease in size: from bulk material, through quantum wells and quantum wires to quantum dots (QDs). In a material world, QDs are structures that provide three-dimensional spatial confinement for charge carriers, resulting in their discrete, atomic-like, energy states. This structure of energy states is very different from the cases of higher dimensions, resulting in a wide range of new carrier's properties that could be used to improve or obtain new optoelectronic devices. To build a quantum information device QD can be used as a system, where the computational goals would be achieved by manipulation of quantum bits (qubits). In conventional devices, a controlled physical system is described as incoherent, which can be altered by changing the intensity of the external field (such as electrical or optical excitation). But if you consider a single qubit, we will have both an amplitude and a phase-controlled by a single pulse at the same time. The aim of quantum control is to use such fields without destroying the fragile quantum state of the system. Additionally, the phase (the coherence) of the qubit has to be conserved during computational manipulations and readout measurements.

The concept of coherent control has already been used in physical research. Here are some examples: photon echo was used to probe the coherence of ensemble of InAs QDs, nuclear magnetic and electron spin resonance spectroscopy; interference of reaction pathways to control photochemical reactions; manipulation of qubits in atomic vapors, ion traps; interference of one- and two-photon absorption for photocurrent generation when no electric field is applied; ultrafast control of excitons in quantum wells for possible use in all-optical switches. New devices based on quantum properties of semiconductor nanoparticles are already built: single-photon source [1], all-optical

quantum gate [2], and entangled photon sources [1, 3].

The biggest part of this paper is a review of scientific techniques used in the study of QDs and is focused on the basic principles of optical coherent control of the exciton. It also considers the key experiments described in the literature and attempts to capture the progress in experimental physics, which took place after the demonstration of coherent optical control of the quantum state of a single QD [4].

2. PHYSICAL PROPERTIES OF SELF-ASSEMBLED QUANTUM DOTS

Nowadays, there are a number of physical systems that provide quantum confinement which results in a discrete electronic energy spectrum. For example, interface fluctuation GaAs/AlGaAs QDs, core-shell CdSe/ZnS nanocrystals fabricated by metallic organic vapor phase epitaxy or by colloidal methods, QDs localized by patterned gate electrodes, and self-assembled QDs grown by Molecular Beam Epitaxy (MBE). Epitaxial method relies on the deposition of new atomic layers of a semiconductor on the host crystal surface [5]. Advanced MBE machines allow monolayer growth precision, which is about 3 Å. QDs of the highest quality are those that are grown by MBE. Self-assembled QDs, e.g. InAs/GaAs, are formed naturally as a result of a phase transition driven by the strain that builds up when two materials with a different lattice constant are grown on one another. GaAs serves as a host matrix, and InAs is deposited on it. Initially, when the InAs total layer thickness is smaller than the critical one, InAs on GaAs surface forms a thin layer which, if then covered again with GaAs, forms a sample with InAs quantum wells. However, due to 7 % difference in the values between the lattice constants of InAs and GaAs a surface tension builds up, and a growth without defects cannot be continued for more than two monolayers of InAs. When the thickness of the

---

* roman.kolodka@gmail.com

InAs-layer exceeds the critical level, material, to release that stress, goes through phase transition forming islands of InAs on the wetting layer. After this GaAs is deposited on the sample to completely cover the InAs islands in order to eliminate defects and unterminated chemical bonds, which provides superior optical properties of the sample.

The shape of the structures grown by MBE can be determined by cross-sectional scanning tunneling microscopy [6], and is typically of a lens-type or a truncated square pyramid. The height and base length are of about 4-5 nm and 18-25 nm respectively. Roughly 10^5 atoms of InAs are locally incorporated into the GaAs matrix, but still, this mesoscopic system exhibits a discrete energy spectrum.

Although the epitaxially self-assembled QDs have very good optical properties, the distributions in size and in-plane location are of a statistical nature. Therefore, each dot has a different shape and composition, and this is reflected in particle's energy levels. A spread of radiation energy and randomness of the nanostructure positioning are, probably, the biggest obstacles in building a scalable qubit system on the basis of semiconductor QDs. But there are reasons for optimism too: a narrow emission energy distribution of less than 10 meV was achieved on the samples manufactured for QD lasers with low threshold [7]; control over the placement of the dots on the pre-patterned matrices [8] is now possible; in the samples with multiple QDs layers grown about each other, anti-crossing behavior of different exciton transitions has been observed [9].

3. EXCITON'S ENERGY SPECTRUM

Localized InAs material has a smaller band gap than the GaAs matrix, therefore it creates a potential well. When the volume of InAs decreases and becomes comparable to the effective Bohr radius, quantum confinement strongly influences the density of energy states. If the dimension is close to zero, the system provides a three-dimensional confinement. In fact, so-called QDs are not zero-dimensional, about 25 nm wide and 5 nm high, measured along the growth direction. The strongest motional confinement is along the growth axis. A QD can be considered now as a system with strong confinement along the z direction, and two-dimensional parabolic confinement in two other directions. To quantify the structure's energy levels the pseudo-potential theory is usually exploited.

A change of the volume of the quantum confinement system makes some corrections to the energy spectrum of the QD in comparison to the bulk material, but the optical selection rules for transitions between QD electron and hole states remain. The QD levels in the conduction band remain twofold spin-degenerated, and the levels in the valence band split into heavy- and light-hole doublets due to strong spatial confinement. From the optical emission point of view, it is important to consider the simplest charge configuration of a QD-neutral exciton X^0. The system consists of a single electron-hole pair in their lowest energy levels. The valence band heavy hole has a spin quantum number J, $J_z = 3/2, \pm 3/2$. The conduction band electron has a spin S, $S_z = 1/2, \pm 1/2$. The total angular momentum of the system can be $\Delta J = \pm 1$ or ± 2. Because a single photon has an angular momentum of ± 1, the only optically active transitions will only be for the states of $\Delta J = \pm 1$: $|\Uparrow\downarrow\rangle$ and $|\Downarrow\uparrow\rangle$. The optically inactive doublet with $\Delta J = \pm 2$ is called "dark", and the exciton with $\Delta J = \pm 1$ is called "bright". The real QD is, as a rule, not symmetrical and this, together with the built strain, causes coherent mix between the bright exciton states. Through electron-hole exchange interaction, the exciton will coherently precess changing the spin states from $+1$ to -1 and back. For self-assembled InAs/GaAs QDs the fine structure splitting is of about 10 μeV [10]. Due to electron-hole exchange interaction and symmetry of the dot, the polarization of the emitted photon will be changed from circular to linear; photons with angular momentum of $+1 (-1)$ ideally would be right (left) circularly polarized, $\sigma+ (\sigma-)$, but now the light will be linearly polarized and denoted as $\pi_X (\pi_Y)$.

Another charge system of a QD is a negatively charged exciton X^{-1} with one hole and two electrons. Due to electron-electron and hole-electron Coulomb interaction the transition energy of the complex will be shifted from X^0 by $\Delta E = E_{ee} - E_{he}$. For InAs/GaAs QDs the energy of this trion transition is lower by 6 meV comparing to neutral exciton. Because of two electrons and one hole the degeneracy of two trion states is not broken and the emitted photon is circularly polarized.

When we consider a "biexciton" (usually denoted as XX, less often as 2X) – two electrons and two holes in the same QD, the emission energy difference comparing to X is found in a similar way ($\Delta E = 2E_{ee} + 2E_{hh} - E_{he}$). For InAs/GaAs QD ΔE is about 2 meV.

Every QD charge complex has a unique spectral signature due to the Coulomb interaction between carriers, and even when every dot has a quite different transition energy, the general energy difference between charged combinations is the same. This is very convenient and helps a lot in the identification of the dot states in the spectrum.

Typical emission energy for most of the semiconductor QDs is in the range of eV, fine structure splitting is denoted in the range of tens of μeV, the characteristic transition linewidth (which cannot be measured directly because of the spectrometer spectral resolution of ⌣ 30 μeV) is ⌣ 1 μeV. The potential well of a dot is from 100 to 300 meV deep in the conduction band, and from 30 to 100 meV deep in the valence band. The wave function's size of a trapped carrier can be calculated from observations of quantum-confined Stark effect [11], or from magneto-tunneling spectroscopy [12]. The size of the electron's wave function is approximately twice the size of the hole's one.

4. OVERVIEW OF EXPERIMENTAL TECHNIQUES

The main challenge when performing experiments with coherent optical control is a separation of a weak signal, conventionally less than one photon at a measuring cycle, from spectrally wide controlling laser pulse of more than 10^4 photons of a similar wavelength and polarization. A number of experimental methods were developed to solve this problem, and the most widely used will be reviewed here now.

4.1 Control of *p*-shell by Measuring the Photoluminescence from *s*-level

The very first experiment on coherent optical control of semiconductor QD states was performed by control of *p*-level excitons [4]. In Fig. 1, a schematic diagram of the concept of measurement is shown, which is similar to the photoluminescence (PL) of excitation. A controlling pulse of a short wavelength excites the optical transitions between the exciton ground state and the first excited state. Absorption creates a *p*-level exciton which then relaxes (in about 40 ps) to the *s*-level state. The *s*-level exciton then recombines releasing a photon of energy, which is about 20 meV lower than the energy of the control pulse. In such a way, the final occupation of the *p*-level is measured.

This method is not very suitable for use in quantum information. The reason is a short coherence time of the *p*-level exciton, which is limited due to the relaxation to *s*-level. That is why there were few reports of experiments using this approach in recent years. However, resonant pulsed excitation of a *p*-level exciton was demonstrated and showed that it can serve as a trigger in a single photons source [13].
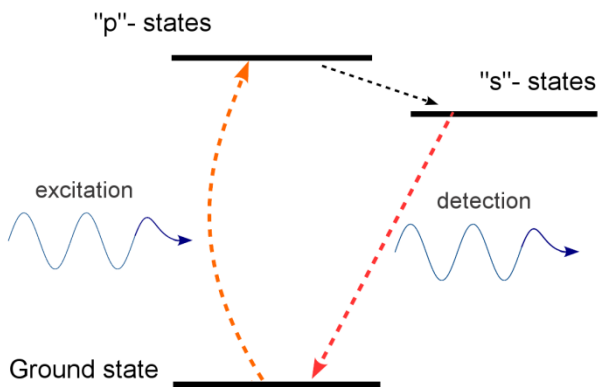

Fig. 1 – Measurement of the photoluminescence from the *s*-level provides a measure of the final *p*-level occupation

4.2 Time-resolved Pump-probe

Pump-probe measurements are the most popular techniques used to resolve in time single QDs that are resonantly excited. Detected signal reflects the third-order optical non-linearity of the dot either in the change of transmission, reflectivity or as the four-wave-mixing of the probe.

In four-wave-mixing experiments, the sample is excited by so-called "pump" and delayed in time "probe" pulses. When the pump hits the sample, it creates an exciton polarization of the first order, which oscillates at the resonant frequencies generated by the system. Probe-pulse comes with a certain time delay after pump and also creates exciton polarization. Exciton polarization of a second-order has a term, which is the result of interference between exciton polarization created by pump- and probe-pulses. In the analogy to Ramsey interference experiments, this is revealed in the population inversion, which oscillates at a frequency that is the difference between those two exciting pulses.

Four-wave mixing experiment's advantage is that the third-order polarization also contains phase infor-

mation. It can be obtained from the heterodyne pump-probe measurements where the signal interferes with the third reference pulse. This provides a direct measurement of the exciton polarization, and hence the optical coherence.

Time-resolved experiments of four-wave-mixing were used with great success for the ensemble of QDs in the study of the internal phase loss of the exciton coherence. In these experiments, to overcome the problem of uneven exciton energy between QDs, photon echo was used [14].

4.3 Photocurrent Technique

To measure the population level of the exciton a QD is embedded into the photodiode. In Fig. 2, a principle of the measurements is illustrated.

All carriers that tunnel from the QD contribute to the measured photocurrent. Thus, the effectiveness of the method for determining the state of exciton using photocurrent is very high; this is the major advantage of the method. High efficiency of the exciton state measurements significantly reduces the duration of the measurement and gives a cleaner data. In the case of optical measurements, only 2 % of the light emitted by the dot can be detected.

Critics of the photocurrent method often argue that because of the need to tunnel the electron from the dot the exciton coherence is decreased. However, the coherence time of 300 ps was measured, which is half of the exciton radiative lifetime [14]. Herewith the effectiveness of that measurement was approximately 50 %. There is a choice between measurement efficiency and a tunneling time. That is, in principle, signal strength can be sacrificed in favor of a longer coherence time, close to the exciton radiative lifetime.
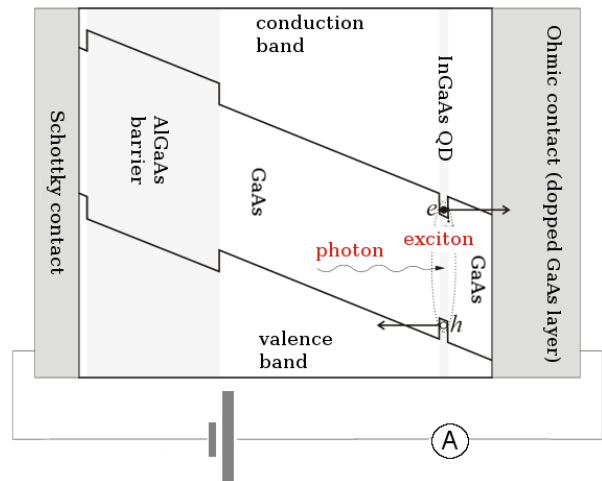

Fig. 2 – Principle of exciton population photocurrent detection. An electric field is applied between the contacts of the photodiode and due to this, the carriers tunnel from the dot. This is reflected in the change of the current (for instance, if the excitation laser repetition rate is 76 MHz, the ΔI will be 12.18 pA)

The photocurrent measurement method has some drawbacks. The first is the background photocurrent, which is proportional to the excitation pulse intensity. It is considered that the reason for this is the absorption of light by other dots that are connected in parallel and

also give a contribution to the photocurrent. The second is the need for high-quality samples, which limits the possibility to study other samples. The other drawback is the fact that the measurement itself is destructive (the better signal we get, the shorter coherence time is).

4.4 Resonant Fluorescence

The biggest problem in all-optical resonant excitation and detection experiments is the separation of the signal photon from the intense laser pulse. One of the most impressive improvements was the implementation of resonant fluorescence detection of the signal. The method uses two laser pulses. The first prepares the system in the condition that is needed and the second one can be used to see what has changed. The second pulse in this case resonantly excites a studied optical transition; an incoherent photon emitted by radiative recombination is then detected.

In the early experiments [19], radiation from the dot was collected perpendicularly to the sample, and controlling/pump pulses fell under large angles. Spatial and polarization filters were used to separate the signal and the scattered laser light. This geometry has predetermined a large size of a laser spot, so big that several QDs were excited at the same time.

Alternative geometry for resonant fluorescence offers to measure the signal along the same direction as the controlling/pump pulse, but with orthogonal polarizations. In this case, the polarizers have to be of very high quality.

5. COHERENT BEHAVIOR OF RESONANTLY EXCITED CADMIUM SELENIDE QUANTUM DOTS

CdSe QDs are widely used in the study of semiconductor nanoparticles. The main reason for such a big interest in CdSe nanocrystals, as well as in a majority of A_2B_6 nanomaterials, is a high quantum yield of radiation-induced electron-hole pairs [20]. Moreover, the most efficient technologies of chemical synthesis are developed exactly for A_2B_6 compounds. In particular, methods of colloidal chemistry, that allows obtaining high-quality nanoparticles in macroscopic quantities at a low cost [21].

Chemical methods of semiconductor nanoparticles synthesis, in particular, CdSe are used very often nowadays. They are relatively cheap in comparison with the methods of Molecular Epitaxy or Pulsed Laser Deposition. It is also possible to obtain a desirable, in a certain range, size of the particles by changing individual parameters of chemical reactions [22].

Studied nanoparticles were held either in a toluene solution or in a dry state. For PL measurements or Raman scattering spectra, as well as for the transmission measurements, the solution with nanoparticles was put on the metal or quartz linings and dried. Recording of the PL and transmission spectra was done using a colloidal solution. Registration of low-temperature PL spectra of nanoparticles was performed when the sample was placed in liquid helium in a superfluid state ($T = 1.6$ K).
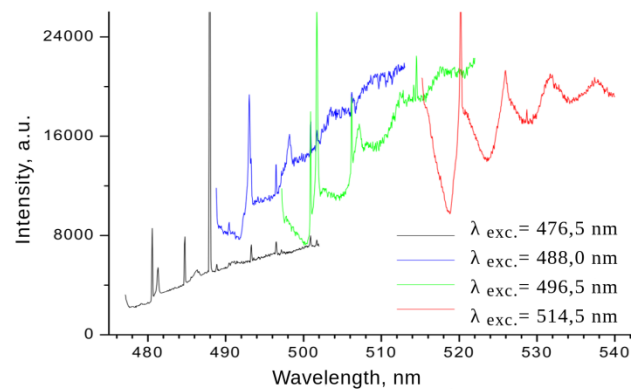

Fig. 3 – Raman spectroscopy spectra and photoluminescence of CdSe nanoparticles at different excitation wavelengths
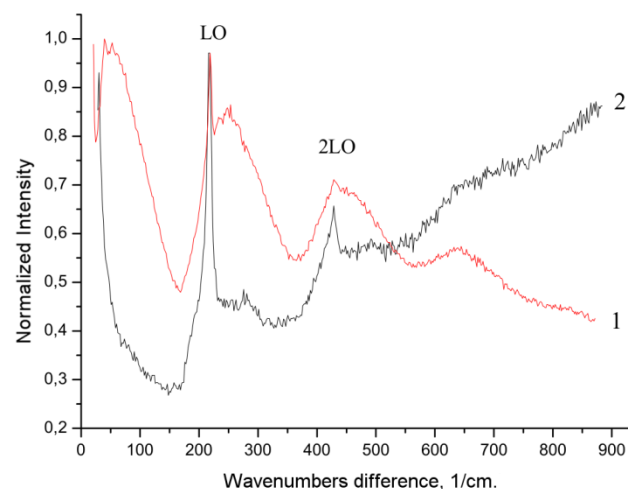

Fig. 4 – Spectra of secondary radiation of CdSe nanoparticles. Black spectrum (denoted as "2") refers to a little bit different type of the sample and is here for comparison only

5.1 Luminescence Properties of CdSe. Stokes Shift

For studied CdSe QDs, a typical PL spectrum consists of two straps: a narrow one that is (spectrally) close to the absorption band, and a lower-energy one that is a result of either admixtures or defects [23]. Slight intensity redistribution between the PL peaks is registered as the temperature changes.

As a rule, full width at half maximum (FWHM) of a luminescence peak is equal to the FWHM of the absorption band and mainly depends on the QDs size distribution. The relevant spectral position of those two peaks is characterized by the Stokes shift. A magnitude of the Stokes shift is quite noticeable for semiconductor nanomaterials [24] and does not change much with temperature. Its value is about 0.15 eV. Probably, the main reason why we witness Stokes shift for an ensemble of nanoparticles that have a fairly broad size distribution is the process of re-absorption, when the particles of a bigger size absorb photons radiated by smaller nanoparticles. Another possible reason for radiation energy reduction in comparison to the absorption energy could be related to the existence of local surface states [25]. This point of view seems quite reasonable because the relative part of surface atoms increases substantially as

the size of nanoparticles decreases.

To study the processes leading to this energy shift, the analysis of the secondary radiation of the CdSe nanoparticles was executed.
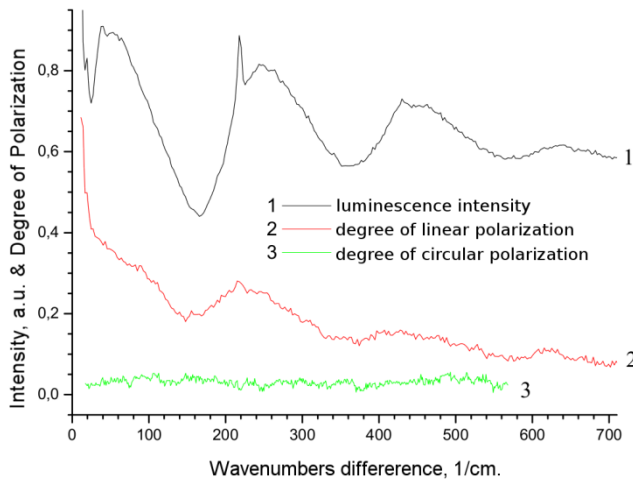

Fig. 5 – Polarization dependence. Correlation with the spectrum of CdSe nanoparticles secondary radiation

5.2 Secondary Radiation

Obtained spectra of CdSe nanoparticles secondary radiation, excited by different wavelengths (Fig. 3), could be differentiated as follows: a broad luminescence background from thermalized excitons, lines of Raman scattering (with the participation of one, two and so on LO-phonons), and a luminescence with characteristic triangular saw-toothed structure. The last-mentioned feature strongly depends on the excitation wavelength.

A change in the intensity of each component of the spectrum, when excited with different wavelengths, is the result of summing up both resonant and non-resonant parts of radiation. As the excitation energy is changed, nanoparticles of different sizes are in resonance, and they are characterized by a different electron transition frequency. In this case, spectra of different sample's secondary radiation look unalike when excited with identical quanta of energy. In Fig. 4, we see the spectra from two different samples both excited at the wavelength of 514.5 nm. The saw-toothed structure is more prominent for one sample, while the other one shows more distinct lines from resonant Raman scattering effect on the thermalized exciton background.

5.3 Coherent Properties

Experimental study of resonantly excited excitons relaxation was conducted at the temperature of 1.6 K because the intensity of non-equilibrium radiation of

CdSe particles decreases with the temperature rise.

For measurements of the polarization spectra, the wavelength $\lambda = 514.5$ nm (Fig. 3) was used; at this condition, we get the best match with the resonant transition.

It is clear from the character of the polarization degree under the resonant linearly polarized excitation (see Fig. 5) that the resonantly excited exciton keeps its dipole momentum oscillation plane for some time. The energy of the exciton and its dipole momentum oscillating plane deviate with time from the set excitation polarization as the relaxation happens.

The degree of linear polarization decreases non-monotonously as we move further from the excitation energy. Positions of the peaks coincide with the PL peaks, and this, probably, denotes that there are two processes of exciton relaxation.

Exciton created in a non-equilibrium state at liquid helium temperatures relaxes quite slowly for us to register radiation from intermediate states. The relaxation is possible via the creation of LO phonons, exciton energy substantially decreases during such relaxation, but the polarization degree remains unchanged when excited by linearly polarized light. Another relaxation process happens simultaneously, probably, through the interaction with acoustic phonons. Since the acoustic phonon energy is substantially lower than the energy of optical phonons, the degree of linear polarization significantly decreases as we move further away from the excitation energy. The result of such stepwise process is a rapid loss of dipole moment oscillations direction that was preset by the polarization of excitation radiation.

This explanation is consistent with the presence of PL band's shift with respect to the absorption. Besides, under the proposed model relaxation of the resonantly excited exciton can be implemented without changing the spin state [27, 28].

From the polarization dependence spectra of the exciton created by linearly and circularly polarized resonant light, we make a conclusion that the studied nanoparticles are able to "remember" only linear polarization, and this corresponds to created exciton's angular momentum of zero.

6. CONCLUSIONS

In this paper, we review the key experimental techniques used in the study of coherent properties of an exciton localized in a quantum dot. For a better understanding, we make a close look on the exiton energy spectrum. Besides this, we demonstrate our results on studies of CdSe quantum dots exciton relaxation at low temperatures. Stokes shift for an ensemble of nanoparticles was observed and was referred to the process of re-absorption. In the spectra of secondary radiation a coherent behavior of the studied excitons was observed.

REFERENCES

1. Z. Yuan, B.E. Kardynal, R.M. Stevenson, A.J. Shields, C.J. Lobo, K. Cooper, N.S. Beattie, D.A. Ritchie, M. Pepper, *Science* **295**, 102 (2002).
2. D. Englund, A. Faraon, I. Fushman, N. Stoltz, P. Petroff, J. Vukovic, *Nature* **450**, 857 (2007).
3. T.M. Stace, G.J. Milburn, C.H.W. Barnes, *Phys. Rev. B* **67**, 085317 (2003).
4. N.H. Bonadeo, J. Erland, D. Gammon, D. Park, D.S. Katzer, D.G. Steel, *Science* **282**, 1473 (1998).
5. E.F. Schubert, *Doping in III-V Semiconductors* (Cambridge: Cambridge University Press: 1993).
6. J.H. Blokland, M. Bozkurt, J.M. Ulloa, D. Reuter, A.D. Wieck,

P.M. Koenraad, P.C.M. Christianen, J.C. Maan, *Appl. Phys. Lett.* **94**, 023107 (2009).

7. H-Y. Liu, I.R. Sellers, T.J. Badcock, D.J. Mowbray, M.S. Skolnick, K.M. Groom, M. Gutierrez, M. Hopkinson, J.S. Ng, J.P.R. David, *Appl. Phys. Lett.* **85**, 704 (2004).

8. P. Atkinson, S. Kiravittaya, M. Benyoucef, A. Rastelli, O.G. Schmidt, *Appl. Phys. Lett.* **93**, 101908 (2008).

9. E.A. Stinaff, M. Scheibner, A.S. Bracker, I.V. Ponomarev, V.L. Korenev, M.E. Ware, M. Doty, T. Reinecke, D. Gammon, *Science* **311**, 636 (2006).

10. M. Bayer, G. Ortner, O. Stern, A. Kuther, A.A. Gorbunov, A. Forchel, P. Hawrylak, S. Fafard, K. Hinzer, T.L. Reinecke, S.N. Walck, J.P. Reithmaier, F. Klopf, F. Schäfer, *Phys. Rev. B* **65**, 195315 (2002).

11. J.J. Finley, M. Sabathil Vogl, G. Absteiter, R. Oulton, A.I. Tartakovskii, D.J. Mowbray, M.S. Skolnick, S.L. Liew, A.G. Cullis, M. Hopkinson, *Phys. Rev. B* **70**, 201308(R) (2004).

12. A. Patané, R.J.A. Hill, L. Eaves C. Main, M. Henini, M.L. Zambrano, A. Levin, N. Mori, C. Hamaguchi, Yu.V. Dubrovskii, E.E. Vdovin, D.G. Austing, S. Tarucha, G. Hill, *Phys. Rev. B* **65**, 165308 (2002).

13. P. Ester, L. Lackmann, S. Michaelis de Vasconcellos, M.C. Hübner, A. Zrenner, M. *Bichler, Appl. Phys. Lett.* **91**, 111110 (2007).

14. P. Borri, W. Langbein, S. Schneider, U. Woggon, R.L. Sellin, D. Ouyang, D. Bimberg, *Phys. Rev. Lett.* **87**, 157401 (2001).

15. A. Zrenner, E. Beham, S. Stufler, F. Findeis, M. Bichler, G. Absteiter, *Nature* **418**, 612 (2002).

16. A.J. Ramsay, R.S. Kolodka, F. Bello W. Fry, W.K. Ng, A. Tahraoui, H.Y. Liu, M. Hopkinson, D.M. Whittaker, A.M. Fox, M.S. Skolnick, *Phys. Rev. B* **75**, 113302 (2007).

17. S. Stufler, P. Machnikowski, P. Ester, M. Bichler, V.M. Axt, T. Kuhn, A. Zrenner, *Phys. Rev. B* **73**, 125304 (2006).

18. S.J. Boyle, A.J. Ramsay, F. Bello, H.Y. Liu, M. Hopkinson, A.M. Fox, M.S. Skolnick, *Phys. Rev. B* **78**, 075301 (2008).

19. K. Kuroda, T. Kuroda, K. Watanabe, T. Mano, K. Sakoda, G. Kido, N. Koguchi, *Appl. Phys. Lett.* **90**, 051909 (2007).

20. D.V. Talapin, A.L. Rogach, I. Mekis, S. Haubold, A. Kornowski, M. Haase, H. Weller, *Colloids Surf A* **202**, 145 (2002).

21. Y. Yan, Y. Li, X. Qian, J. Yin, Z. Zhu, *Mater. Sci. Eng. B* **103**, 202 (2003).

22. Yu.Yu. Bacherikov, M.O. Davydenko, A.M. Dmytruk I.M. Dmitruk, P.M. Lytvyn, I.V. Prokopenko, V.R. Romanyuk, *SPQEO* **9** 2, 75 (2006).

23. S.A. Blanton, M.A. Hines, P. Guyot-Sionnest, *Appl. Phys. Lett.* **69**, 3905 (1996).

24. A. Franceschetti, S.T. Pantelides, *Phys. Rev. B* **68**, 033313 (2003).

25. R.W. Meulenberg, T. Jennings, G.F. Strouse, *Phys. Rev. B* **70**, 235311 (2004).

26. M.G. Bawendi, W.L. Wilson, L. Rothberg P.J. Carroll, T.M. Jedju, M.L. Steigerwald, L.E. Brus, *Phys. Rev. Lett.* **65**, 1623 (1990).

27. E.L. Ivchenko, *Pure Appl. Chem.* **67** 3, 463 (1995).

28. Al.L. Efros, M. Rosen, M. Kuno, M. Nirmal, D.J. Norris, M. Bawendi, *Phys. Rev. B* **54**, 4843 (1996).

Вивчення когерентних властивостей екситону в напівпровідникових квантових точках

Р.С. Колодка, І.П. Пундик, І. Дмитрук

*Фізичний факультет, Київський національний університет імені Тараса Шевченка,
проспект академіка Глушкова 2/1, 03127 Київ, Україна*

У цій роботі ми робимо огляд експериментальних методик, що використовуються при вивченні напівпровідникових квантових точок, та акцентуємо увагу на основних принципах оптичного когерентного управління екситоном. Ми обговорюємо як оптичні методи дослідження (часороздільний памп-проб, контроль p-оболонки шляхом вимірювання фотолюмінесценції з s-оболонки, резонансна флюоресценція), так і фотоструму. Останній хоч і зменшує когерентність системи, але дозволяє її охарактеризувати кількісно. Особлива увага приділяється фізичним властивостям самоорганізованих квантових точок, оскільки сучасні методи їх виготовлення дозволяють отримати високоякісні наночастинки в макроскопічних кількостях. Також ми обговорюємо наші результати, отримані в процесі вимірювань спектрів випромінювання та поглинання колоїдних квантових точок CdSe. Спостерігається зсув Стокса для ансамблю наночастинок, що мають досить великий розподіл за розміром. Зроблено аналіз вторинного випромінювання наночастинок CdSe для вивчення процесів, що призводять як до цього енергетичного зсуву, так і до втрати екситоном поляризації.

Ключові слова: Квантові точки, Екситон, Наночастинки, Когерентне управління, Релаксація.